

# Lidar Sensors for Autonomous Landing and Hazard Avoidance

Farzin Amzajerdian<sup>1</sup>, Larry B. Petway<sup>1</sup>, Glenn D. Hines<sup>2</sup>, Vincent E. Roback<sup>3</sup>, and Robert A. Reisse<sup>4</sup>  
*NASA Langley Research Center, Hampton, Virginia, 23681*

Diego F. Pierrottet  
*Coherent Applications, Inc., Hampton, Virginia, 23666*

## ABSTRACT

**Lidar technology will play an important role in enabling highly ambitious missions being envisioned for exploration of solar system bodies. Currently, NASA is developing a set of advanced lidar sensors, under the Autonomous Landing and Hazard Avoidance (ALHAT) project, aimed at safe landing of robotic and manned vehicles at designated sites with a high degree of precision. These lidar sensors are an Imaging Flash Lidar capable of generating high resolution three-dimensional elevation maps of the terrain, a Doppler Lidar for providing precision vehicle velocity and altitude, and a Laser Altimeter for measuring distance to the ground and ground contours from high altitudes. The capabilities of these lidar sensors have been demonstrated through four helicopter and one fixed-wing aircraft flight test campaigns conducted from 2008 through 2012 during different phases of their development. Recently, prototype versions of these landing lidars have been completed for integration into a rocket-powered terrestrial free-flyer vehicle (Morpheus) being built by NASA Johnson Space Center. Operating in closed-loop with other ALHAT avionics, the viability of the lidars for future landing missions will be demonstrated. This paper describes the ALHAT lidar sensors and assesses their capabilities and impacts on future landing missions.**

## I. Introduction

Missions to solar systems bodies must meet increasingly ambitious objectives requiring highly reliable “soft landing”, “precision landing”, and “hazard avoidance” capabilities. Robotic missions to the Moon and Mars demand landing at pre-designated sites of high scientific value near hazardous terrain features, such as escarpments, craters, slopes, and rocks. Missions aimed at paving the path for colonization of the Moon and human landing on Mars need to execute onboard hazard detection and precision maneuvering to ensure safe landing near previously deployed assets. Asteroid missions require precision rendezvous, identification of the landing or sampling site location, and navigation to the highly dynamic object that may be tumbling at a fast rate. Lidar technology will play a major role in enabling these ambitious mission concepts due to its capabilities of precision measurement of vehicle relative proximity and velocity, and providing high resolution elevation map of the surface during the descent to the targeted body.

Currently, NASA Langley Research Center (LaRC) is developing a set of novel lidar sensors under the Autonomous Landing and Hazard Avoidance Technology (ALHAT) project<sup>1</sup>. These lidar sensors are 3-Dimensional Imaging Flash Lidar, Doppler Lidar, and Laser Altimeter. These three lidar sensors perform five essential landing functions: Altimetry, Velocimetry, Terrain Relative Navigation (TRN), Hazard Detection and Avoidance (HDA) and Hazard Relative Navigation (HRN). The operation of these advanced lidar sensors may be best described in the context of a lunar landing scenario as shown in Fig. 1. As the landing vehicle initiates its powered descent toward the landing site at about 20 km above the surface, the Laser Altimeter begins its operation providing altitude data

---

<sup>1</sup> Laser Remote Sensing Branch, Engineering Directorate, NASA Langley Research Center, Mail Stop 468.

<sup>2</sup> Flight Software Systems Branch, Engineering Directorate, NASA Langley Research Center, Mail Stop 472.

<sup>3</sup> Remote Sensing Flight Systems Branch, Engineering Directorate, NASA Langley Research Center, Mail Stop 468.

<sup>4</sup> Flight Projects Directorate, NASA Langley Research Center, Mail Stop 494.

with sub-meter precision. This measurement will reduce the vehicle position error significantly since the Inertial Measurement Unit (IMU) suffers from drastic drift over the travel time from the Earth. The IMU drift error can be over 1 km for a Moon-bound vehicle and over 10 km for Mars. Accurate altitude data reduces position error to a few hundred meters. Shortly after, the Flash Lidar starts its operation by having its laser beam focused to illuminate a subset of its pixels generating a relatively low-resolution elevation data of the terrain below. The reason for reducing the divergence of the lidar transmitter beam to a fraction of its receiver field of view is to increase its operational range to about 15 km from a nominal 1 km. At this altitude, the Flash Lidar can generate elevation maps of the terrain and match them to on-board maps having known surface features such as craters. This process, referred to as Terrain Relative Navigation, will further reduce the vehicle relative position error from hundreds of meters to tens of meters. When the landing vehicle descends to about 2.5 km, the Doppler lidar initiates its operation by providing ground-relative vector velocity and altitude data with high precisions of the order of 1 cm/sec and 10 cm, respectively. The Doppler lidar data will enable navigation to the selected landing site to better than a meter in precision. From about 1 km to 0.5 km from the ground, the Flash Lidar will operate with its full field of view, generating a high resolution elevation map of the landing zone while identifying hazardous features such as rocks, craters, and steep slopes. This elevation map is then processed to determine the most suitable safe landing location (HDA function). The Flash lidar will then continue to update the map in order to establish a trajectory toward the selected landing location. This phase of Flash Lidar operation is referred to as Hazard Relative Navigation. The Flash Lidar operation ceases at approximately 100 m above the ground before the vehicle thrusters create a dust plume. The high precision velocity and altitude data provided by the Doppler Lidar allows the Guidance, Navigation, and Control system to direct the vehicle to the identified landing site and ensure a safe and smooth landing.

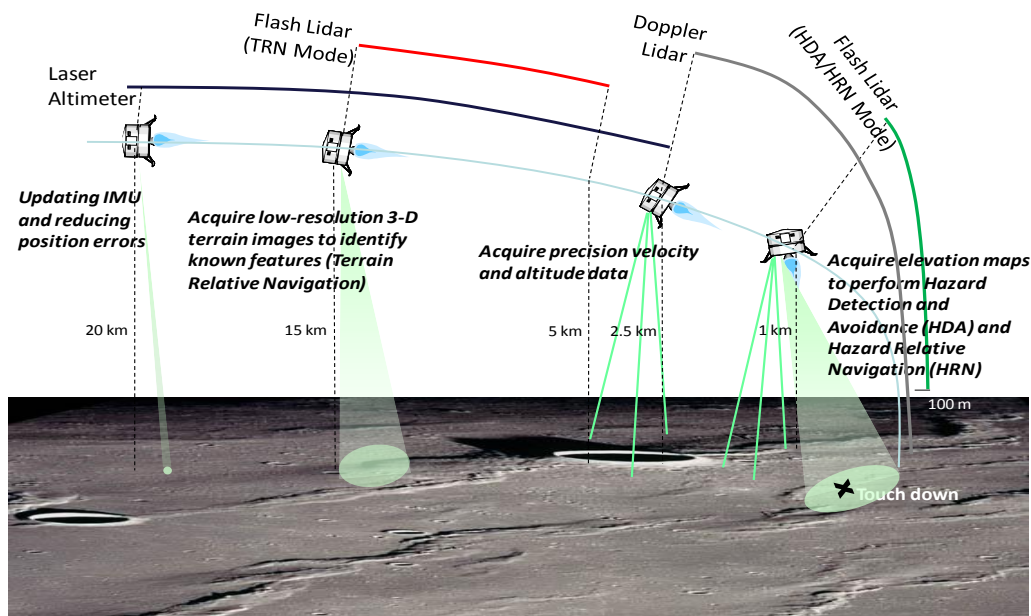


**Figure 1. Lunar Landing Operational Scenario of Lidar Sensors.**

Table 1 below summarizes the functions that each lidar sensor is capable of performing along with their associated operational altitudes during the descent, terminal approach, and landing phases. There is a significant overlap in capabilities of these three lidar sensors. The Flash Lidar is capable of performing all the functions with exception of velocimetry that is provided the Doppler Lidar. The ability of the Doppler Lidar to provide velocity data to better than 1 cm/sec is highly attractive for precision landing. Additionally, the Doppler Lidar provides high resolution altitude and ground-relative attitude data that may further improve precision navigation to the identified landing site. The Laser Altimeter provides independent altitude data over a large operational altitude range from 20 km to 100 m. Although the Flash lidar is fully capable of providing the necessary altitude data, the Laser Altimeter is used in the operational scenario of Fig. 1 in order to lessen spacecraft accommodation issues. Since the orientation of the spacecraft will be different during different phases of descent and landing, it may be difficult to accommodate the Flash Lidar such that it will have a clear view of the ground during the approach phase (< 2km altitude), when it needs to perform HDA and HRN functions, as well as powered descent phase (20 km – 10 km altitude), when

Altimetry and TRN functions need to be performed. Therefore, the Laser Altimeter can reduce the complexity of spacecraft accommodation design and ease the spacecraft attitude control requirements. Even if the Flash lidar can operate over the entire powered descent phase, the Laser Altimeter may serve as a redundant sensor for either or both Altimetry and TRN functions.

**Table 1. Landing lidar sensors and their functions.**

Sensor	Function	Operational Altitude Range
Flash Lidar	HDA/HRN	1000 m – 100 m
	TRN	15 km – 5 km
	Altimetry <sup>1</sup>	20 km – 100 m
Doppler Lidar	Velocimetry	2500 m – 10 m
	Altimetry	2500 m – 10 m
Laser Altimeter	Altimetry	20 km – 100 m
	TRN <sup>1</sup>	15 km – 5 km

<sup>1</sup> Secondary function, maybe considered as redundancy option.

The nominal operational scenario described above will vary depending on the mission and its Entry, Descent, and Landing (EDL) system design. A lunar mission may only require TRN function for meeting its landing ellipse accuracy requirements while another may only need the Doppler Lidar for precision navigation during terminal descent phase and execution of a soft touchdown. On the other hand, a Mars landing mission is very different from Moon landing because of presence of atmosphere and larger gravity force. Other factors that greatly influence the architecture of the sensors suite and its operational characteristics are landing accuracy, landing site terrain features, and the vehicle size. For example, an un-guided parachute descent with large swings and a protective heat-shield will restrict the operational periods of the lidar sensors that must have a clear view of the ground. Asteroid missions are yet very different from the Moon and Mars, as the primary objectives of the sensors are to generate elevation map of the object and measure the vehicle relative bearings in addition to precise proximity and velocity data.

## II. Lidar Sensor Technology Development Approach

NASA-LaRC has been advancing the lidar technology for autonomous safe landing applications from design concepts to operational prototype systems under the ALHAT project for the past 7 years. The capabilities of each of the three lidar sensors were assessed and their performance were characterized through a series of static and dynamic experiments at the NASA-LaRC lidar test range, and from helicopter and fixed-wing aircraft platforms.<sup>2-6</sup> Table 2 lists the aircraft field tests conducted during different technology development phases of the lidars. The scope of each field test expanded as the lidar systems development progressed in order to show their operation as integrated sensor with other ALHAT landing system components, namely the Hazard Detection System (HDS)<sup>7</sup>, developed by NASA Jet Propulsion Laboratory (JPL) and the Autonomous Guidance, Navigation, and Control (AGN&C) system developed by NASA Johnson Space Center (JSC) and Charles Draper Laboratory (CDL). The HDS controls the Flash lidar pointing to the landing site and processes the lidar 3D image frames to select the landing location. HDS then provides the selected landing location coordinates to the AGN&C that uses the Doppler lidar and Laser Altimeter data to navigate the vehicle towards the landing location and execute the touch down maneuver. HDS compute element also uses the Flash lidar and Laser Altimeter data to perform the HRN and TRN functions that improve the vehicle relative position knowledge as described in previous section.

**Table 2. Field tests conducted over the course of lidar sensors development.**

Field Test	Platform	Sensors	Objective	Date
1	A-Star Helicopter	Flash Lidar	<ul style="list-style-type: none"> <li>HDA demonstration</li> </ul>	05/2008
2	A-Star Helicopter	Doppler Lidar	<ul style="list-style-type: none"> <li>Velocity, altitude, attitude demonstration</li> </ul>	08/2008

3	B-200 Airplane	Flash Lidar Laser Altimeter	<ul style="list-style-type: none"> <li>• TRN demonstration</li> </ul>	06/2009
4	Sikorsky S-64 Helicopter (Sky Crane)	Flash Lidar Doppler Lidar Laser Altimeter	<ul style="list-style-type: none"> <li>• Breadboard systems assessments</li> <li>• HDA/HRN Algorithms and NAV Filter tests</li> </ul>	07/2010
5	Bell UH-1H Iroquois (Huey) helicopter	Flash Lidar Doppler Lidar Laser Altimeter	<ul style="list-style-type: none"> <li>• Prototype systems assessment</li> <li>• Integrated operation with HDS and AGN&amp;C</li> </ul>	12/2012

Field tests 1-4 provided invaluable data for the development of fully autonomous prototype systems that were demonstrated in field test 5 campaign (see Fig. 2). The prototype lidars sensors are air-cooled and engineered to be as compact and robust as possible within the project budget and schedule constraints. Prior to field test 5, the prototype lidars were integrated with the HDS and AGN&C, and tested in a dynamic environment at NASA-LaRC Lidar Test Range on an instrumented truck. Operating as integrated sensors with other ALHAT subsystems, the prototype systems performed reliably during the two-week flight test 5 campaign. The prototype lidars were later integrated into a rocket-powered, terrestrial flight-test vehicle. The test vehicle, referred to as Morpheus<sup>8</sup>, is being built by NASA Johnson Space Center (JSC) to demonstrate advanced propulsion and GN&C technologies for future landing missions. A series of integration tests were conducted to validate their interfaces and operational procedures. These integration tests included two tethered tests during which the lidars were activated to communicate and provide data to various avionics while the Morpheus vehicle was suspended from a crane and executing a controlled flight procedure. The integration tests were in preparation for a full landing demonstration in 2014 at a simulated lunar terrain site consisting of realistic hazard features and a few safe landing areas<sup>9</sup>. The lidars will be operating in a closed-loop with the ALHAT HDS and AGN&C to demonstrate autonomous safe landing system that controls the vehicle flight trajectory to the selected safe site and executes the landing maneuver (Fig. 3). The following sections describe each of these advanced lidar sensors and provide their capabilities in their current prototype configuration.

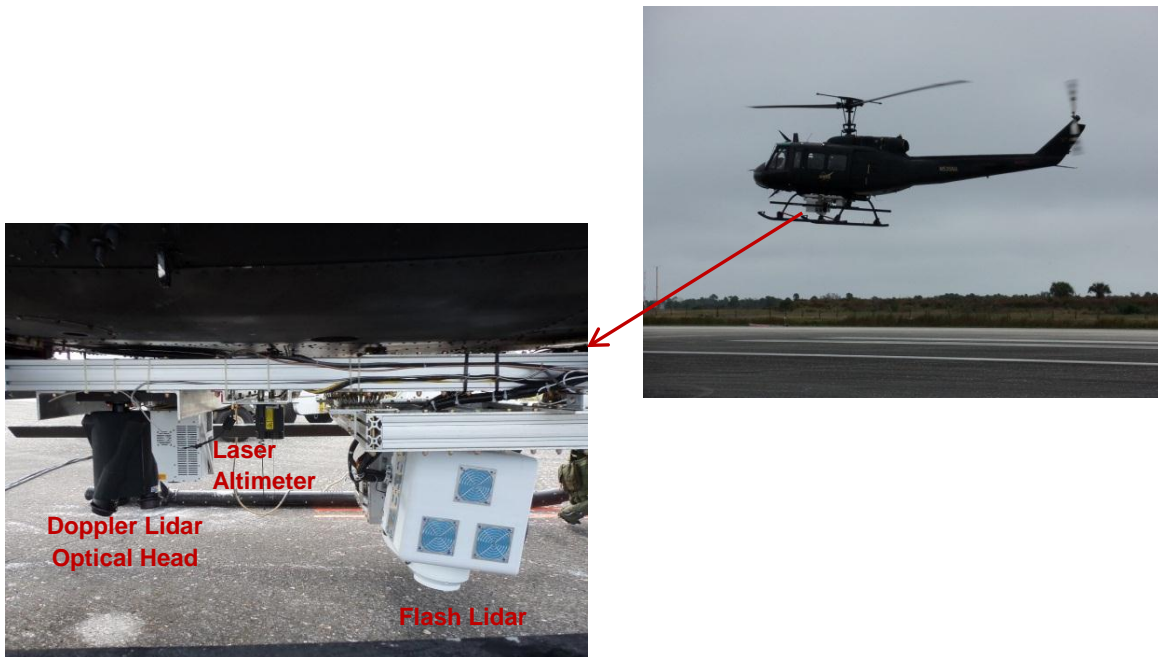


**Figure 2. Prototype lidar sensors mounted under a Huey helicopter during Filed Test 5. The Flash lidar and Doppler lidar electronic chassis are placed in a rack inside the cabin.**

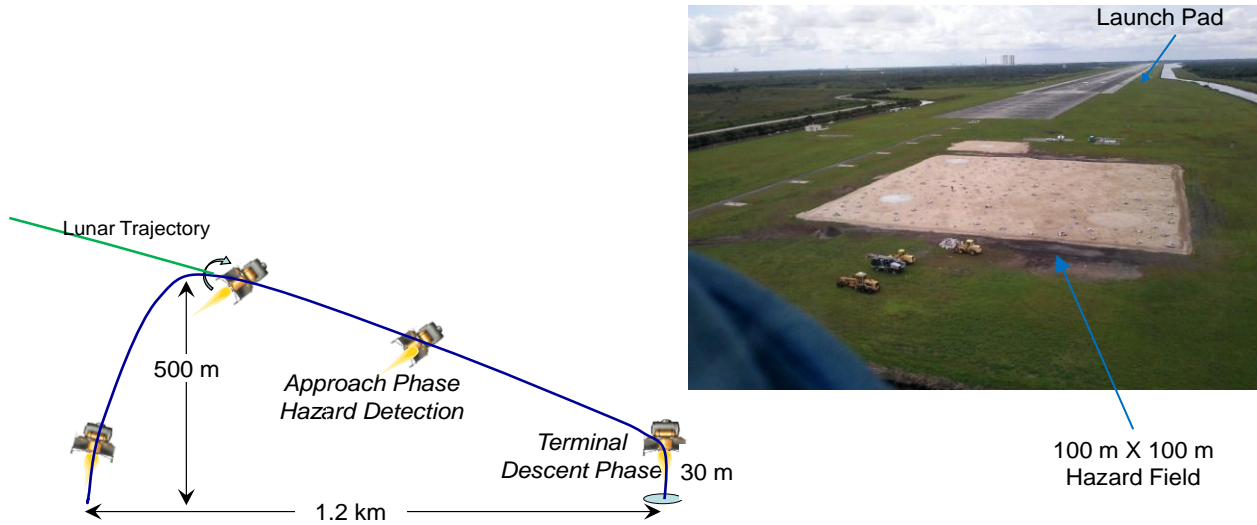


**Figure 3. Closed-loop demonstration of ALHAT landing system using Morpheus vehicle is planned for early 2014 at NASA Kennedy Space Center Lidar. Lidar sensor systems, operating with other ALHAT components as an integrated landing system, will aid autonomous landing at a safe location among hundreds of rock piles and craters.**

### III. 3-Dimensional Imaging Flash Lidar

Flash lidar is capable of generating three dimensional (3D) images of the terrain at video rate with sufficient lateral resolution and range precision for performing landing TRN, HDA, and HRN functions. Flash lidar, as illustrated in Fig. 4, uses a two dimensional detector array to detect a laser pulse return from the target. The detector's Readout Integrate Circuit (ROIC) measures the laser pulse time of arrival of each individual pixel simultaneously. Thus each flash of the laser generates a 3D image of the target illuminated by the laser beam. In older, more conventional imaging lidar systems, the laser beam is scanned over the targeted area in a raster pattern and a single detector is used to detect consecutive pulses. Thus many laser pulses are required to cover the target area and generate a multi-pixel image with sufficient resolution. The major challenge with such a scanning system is controlling the laser beam pointing from a moving platform and then estimating the laser spot position in the target area for each transmitted pulse. By recording a full 3D image with a single laser pulse, Flash lidar allows a much a higher image frame rate, eliminates the need for fast laser beam scanning mechanism, and mitigates the effects of the platform motion.

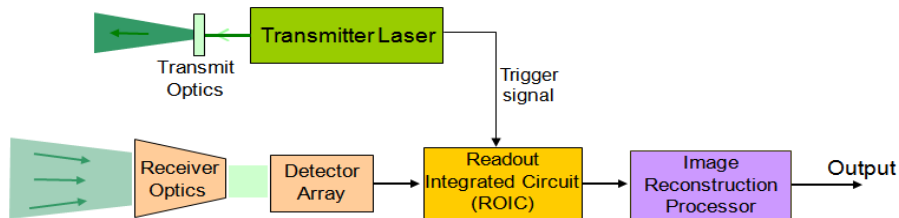


**Figure 4. Schematic of Flash lidar sensor system.**

The Flash lidar developed for ALHAT uses a 3D imaging camera, also referred to as sensor engine, developed by Advanced Scientific Concepts (ASC)<sup>10,11</sup>. The sensor engine consists of a detector array integrated with a matching ROIC packaged with associated detector/ROIC supply and control electronics and a real-time processor that calibrates the output of the ROIC and outputs both range and intensity image frames. The ASC sensor engine has a 128x128 pixel array that is capable of generating real-time images at up to 30 frames per second. Fig. 5 shows the prototype Flash lidar consisting of a sensor head and an electronic chassis. The sensor head houses the sensor engine, the transmitter laser, and the transmit/receive optics, while the sensor Controller and Data Handling (C&DH) unit, the laser driver, the power conditioning/distribution unit, and temperature control boards are housed in the electronic box. The transmitter laser operating at 1.06 micron wavelength, developed by Fibertek, generates a

uniform square shape beam matching the detector array, with a divergence adjusted to match the receiver field of view. The lidar C&DH unit performs a number of function including controlling and monitoring various lidar components, interfacing with avionics, and performing image processing and conditioning. C&DH executes a median filter algorithm for eliminating sporadic range noises, masks the known bad pixels, and applies an absolute range calibration routine. The Flash lidar system and performance specifications are summarized in Table 3. It is worth noting that the current designs of all three prototype sensor systems can be optimized to further reduce their size, mass, and power for integration into landing vehicles. The heat dissipation and thermal control subsystem account for a significant fraction of the size, mass, and power of current systems.



**Figure 5. Prototype Flash lidar sensor.**

**Table 3. Specifications of Flash Lidar Prototype System.**

Parameter		Value
Array Size		128X128
Operational Wavelength		1.06 micron
Laser Pulse energy		45 mJ
Laser Pulsewidth		8 nsec
Receiver Aperture Diameter		100 mm
Receiver Field of View		1 deg. and 5deg.
Frame Rate		20 Hz
Max operational range		1500 m @ 90° look angle
		750 m @ 30° look angle
Range Precision		8 cm
Dimensions	Sensor Head	11.25"x13.5"x13.25"
	Electronics	9.5"x14.2"x13.0"
Weight	Sensor Head	35.5 lbs
	Electronics	36 lbs

#### IV. DOPPLER LIDAR

The ability of Doppler lidar in providing accurate vehicle vector velocity and altitude is critical for establishing a surface inertial navigation fix during the approach phase and navigating the vehicle, with the necessary precision of about 1 m, to the safe landing location identified by the Flash lidar and HDS. Doppler lidar also provides ground relative attitude angles (pitch and roll) that may help with the terminal descent and touch down maneuvers.

The Doppler lidar transmits three laser beams which are separated 120 degrees from each other in azimuth and are pointed 22.5 degrees from nadir. The signal from each beam provides the platform velocity and range to the ground along the laser line-of-sight (LOS). The LOS velocity and range precisions of the lidar have been measured to be approximately 3 mm/sec and 17 cm respectively. The six LOS measurements are then used to derive the three components of the vehicle velocity vector, and its altitude and attitude relative to the ground below. Past landing missions, including Surveyor, Apollo, Viking, Phoenix, and Mars Science Laboratory,<sup>12,13</sup> relied on radar technology for the altitude and velocity data. Doppler lidar offers major benefits including lower mass and smaller size, higher precision and data rate, and much lower false alarm rates. These attributes are particularly critical when autonomous hazard avoidance is employed or when “pinpoint landing” is required.

The Doppler Lidar obtains high-resolution range and velocity information from a frequency modulated continuous wave (FMCW) laser waveform whose instantaneous frequency is modulated linearly with time. Fig. 6 shows the modulation waveform consisting of three segments: up-ramp chirp, constant frequency, and down-ramp chirp. The resultant returned waveform from the target is delayed by  $t_d$ , the light round trip time. When the target or the lidar platform is not stationary during the beam round trip time, the returned waveform will be also shifted up or down, depending on the velocity direction, due to the Doppler effect. When mixing the two waveforms at the detector, an interference signal is generated whose frequency is equal to the difference between the transmitted and received frequencies. In absence of velocity along the laser beam, the signal frequency during the “up-ramp” and “down-ramp” periods are equal and their magnitude is directly proportional to the distance to the target. When the vehicle is moving, the up-ramp and down-ramp frequencies will not be equal and their difference is related to the Doppler velocity. The target range and magnitude of the velocity component along the laser beam are determined through the following simple equations:

$$R = \left(\frac{TC}{2B}\right) \left(\frac{f_{IF}^+ - f_{IF}^-}{2}\right) \quad V = \left(\frac{\lambda}{2}\right) \left(\frac{f_{IF}^+ + f_{IF}^-}{2}\right)$$

where  $f_{IF}^+$  and  $f_{IF}^-$  are the intermediate up-ramp and down-ramp frequencies,  $B$  is the modulation bandwidth,  $T$  is the waveform period,  $C$  is the speed of light, and  $\lambda$  is the laser wavelength.

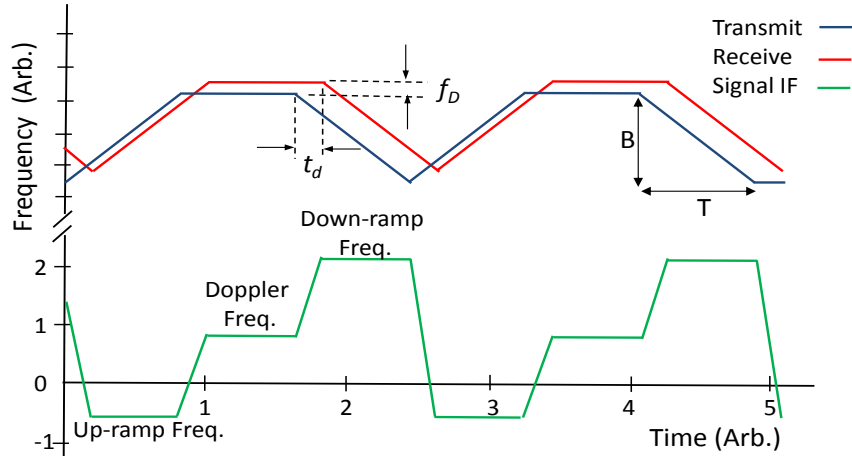


**Figure 6. Linearly frequency modulated transmitted beam and returned signal, and the resulting intermediate frequency (IF) of the homodyne signal.**

The constant frequency segment also produces the Doppler velocity that can be used for eliminating the data dropouts when either up-ramp or down-ramp intermediate frequency is very close to zero and allows for minimizing the measurement ambiguities that may arise in certain scenarios.

Fig. 7 illustrates the system design utilizing an optical homodyne configuration. A relatively low power, single frequency laser operating at eye safe wavelength of 1.55 micron, is used as the master oscillator. The output of this laser is modulated per the waveform of Fig. 6. Part of the laser output is amplified to be transmitted and the remaining is used as the local oscillator (LO) for optical homodyne detection. The lidar transmits three laser beams in different directions and the returns are directed to three corresponding receivers.

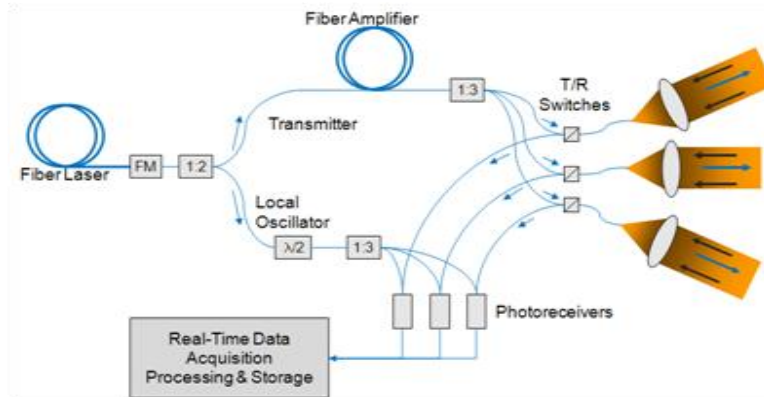


**Figure 7. Doppler lidar system configuration illustrating three transmitted beams and their corresponding receivers providing line-of-sight velocity and range measurements in three different directions.**

The advancement of the Doppler lidar technology under the ALHAT project has led to development of a prototype system shown in Fig. 8. The prototype system consists of an electronics chassis and an optical head that houses the three transmit and receive lenses. All the lidar components, including transmitter laser, receiver, and real-time processor, are housed in the electronic chassis. The optical head is mounted rigidly on the vehicle with a clear field-of-view to the ground, and connected to the electronic chassis through a long fiber optic cable carrying the transmitted beams to the lenses and directing the collected signals from the same lenses to the receivers. The specifications of the prototype Doppler lidar are summarized in Table 4. As noted earlier, a significant fraction of the size, mass, and power is allocated to heat dissipation and temperature control.



**Figure 8. Prototype Doppler lidar system consisting of an electronic chassis and an optical head.**

**Table 4. Specifications of Doppler Lidar Prototype System.**

Parameter	Prototype Lidar
-----------	-----------------



Line-Of-Sight Velocity Error		0.2 cm/sec
Line-Of-Sight Range Error		17 cm
Attitude Error		0.4 deg
Maximum Operational Altitude		2200 m
Data Rate		20 Hz
Operational Wavelength		1.56 micron
Dimensions	Elect. Chassis	17" x 15" x 6"
	Optical Head	8" dia x 10" H
Mass	Elect. Chassis	49 lb
	Optical Head	11 lb
Power		145 W

### V. Laser Altimeter

The vehicle altitude can be measured by the Flash Lidar at high altitudes of over 20 km and the Doppler Lidar from about 2 km above the ground. However, a separate Laser Altimeter sensor can ease the spacecraft design and provide redundancy to this critical data. The prototype Laser Altimeter operates at an eye safe energy level at 1.57 micron wavelength for easier terrestrial operation and testing. The prototype system, as shown in Fig. 9, is significantly more powerful and more precise than ALHAT project desired (Table 1) and it exceeds the performance requirements of any foreseeable landing mission. Altitude measurements with 0.5 m precision from about 20 km is more than sufficient for mitigating the drift by the Inertial Measurement Unit (IMU) and providing an accurate vehicle position estimate. Performing TRN function, using the Laser Altimeter measurements of the terrain contour, requires similar operational range and precision specifications. The current sensor exceeds these performance requirements by more than an order of magnitude. Table 5 lists the physical and performance specifications of the Laser Altimeter prototype. The size, mass, and power of this sensor can be reduced even more significantly than the Flash lidar and the Doppler lidar since we can use a much smaller laser and receiver aperture in development of a space flight unit.



Figure 9. Prototype Laser Altimeter sensor system

Table 5. Specifications of Laser Altimeter Prototype System.

Parameter	Prototype Lidar
-----------	-----------------

Max Operational Range	50 km in atm., 4000 km without atm.
Accuracy	0.0034%
Precision	5 cm
Data Update Rate	30 Hz
Operational Wavelength	1.57 micron
Dimensions	10.25" x 8.75" x 6.5"
Mass	24 lb
Power (28 VDC)	70 W

## VI. Conclusion

Lidar has been identified by NASA as a key technology for enabling autonomous precision safe landing of future robotic and crewed lunar landing vehicles. NASA-LaRC is developing three laser/lidar sensor systems under the ALHAT project. The capabilities of these Lidar sensor systems were evaluated through a series of static tests using a calibrated target and through dynamic tests aboard helicopters and a fixed wing aircraft. The airborne tests were performed over Moon-like terrain in the California and Nevada deserts. These tests provided the necessary data for the development of signal processing software, and algorithms for hazard detection and navigation. The tests helped identify technology areas that need improvement and guide ongoing technology advancement activities.

## Acknowledgments

The authors are grateful to ALHAT project manager, Chirold Epp, NASA Johnson Space Center, for his guidance and support. We also would like to thank NASA's Advanced Exploration Systems (AES) program office for their continued support. The authors also acknowledge the ALHAT team members from NASA Johnson Space Center and NASA Jet Propulsion for their collaboration, and Gregory Gaddis for facilitating the field test at NASA Kennedy Space Center.

## References

1. Epp, C. D., Robinson, E. A., and Brady, T., "Autonomous Landing and Hazard Avoidance Technology (ALHAT)", Proc. of IEEE Aerospace Conference, paper no. 1644, 2008.
2. Pierrottet, D. F., Amzajerjian, F., Meadows, B. L., Estes, R. F., Noe, A. M., "Characterization of 3-D imaging lidar for hazard avoidance and autonomous landing on the Moon," Proc. of SPIE Vol. 6550, 2007.
3. Bulyshev, A., Pierrottet, D. F., Amzajerjian, F., Busch, G. E., Vanek, M. D., and Reisse, R. E., "Processing of three-dimensional flash lidar terrain images generating from an airborne platform," Proc. SPIE Vol. 7329, 2009.
4. Amzajerjian, F., Vanek, M. D., Petway, L. B., Pierrottet, D. F., Busch, G. E., Bulyshev, A., "Utilization of 3-D Imaging Flash Lidar Technology for Autonomous Safe Landing on Planetary Bodies," SPIE Proceeding Vol. 7608, paper no 80, 2010.
5. Roback, V. E., Bulyshev, A., Amzajerjian, F., Brewster, P. F., Barnes, B. W., Kempton, K. S., and Reisse, R. E., "Helicopter Flight Test of 3-D Imaging Flash LIDAR Technology for Safe, Autonomous, and Precise Planetary Landing," Proc. of SPIE, Vol. 8731, SPIE Defense Security, and Sensing Conference, 2013.
6. Pierrottet, D. F., Amzajerjian, F., Petway, L. B., Barnes, B. W., Lockard, G., and Hines, G. D., "Navigation Doppler Lidar Sensor for Precision Altitude and Vector Velocity Measurements Flight Test Results." SPIE Defense and Security Symposium, Orlando, FL, (2011).
7. Huertas, A., Johnson, A. E., Werner, R. A., Maddock, R. A., "Performance Evaluation of Hazard Detection and Avoidance Algorithms for Safe Lunar Landings," Proc. IEEE Aerospace Conference, PP 1-20, 2010.
8. Project Morpheus Website <http://morpheuslander.jsc.nasa.gov>

9. Rutishauser, D., Epp, C. D., and Robertson, E. A., "Free-Flight Terrestrial Rocket Lander Demonstration for NASA's Autonomous Landing and Hazard Avoidance Technology (ALHAT) System," Proc. of AIAA SPACE 2012.
10. Stettner, R., Bailey, H., and Silverman, S., "Three Dimensional Flash Ladar Focal Planes and Time Dependent Imaging," International Symposium on Spectral Sensing Research, Bar Harbor, Maine, 2006.
11. Stettner, R., "Compact 3D Flash LIDAR video cameras and applications," Proc. of SPIE Vol. 7684, 768405, 2010.
12. Pollard, B. D., and Chen, C. W., "A Radar Terminal Descent Sensor for the Mars Science Laboratory Mission," IEEE Aerospace Conference, paper no.1597, 2008.
13. Braun, R. D. and Manning, R. M., "Mars Exploration Entry, Descent and Landing Challenges" I Aerospace Conference, paper no.0076, 2005.